Constraints on the CKM angle γ in $B^0 \to \bar{D}^0 K^{*0}$ and $B^0 \to D^0 K^{*0}$ from a Dalitz analysis of D^0 and $\bar{D}^0$ decays to $K_S \pi^+ \pi^-$

B. Aubert,[1] M. Bona,[1] Y. Karyotakis,[1] J. P. Lees,[1] V. Poireau,[1] X. Prudent,[1] V. Tisserand,[1] A. Zghiche,[1] J. Garra Tico,[2] E. Grauges,[2] L. Lopez,[3] A. Palano,[3] M. Pappagallo,[3] G. Eigen,[4] B. Stugu,[4] L. Sun,[4] G. S. Abrams,[5] M. Battaglia,[5] D. N. Brown,[5] J. Button-Shafer,[5] R. N. Cahn,[5] R. G. Jacobsen,[5] J. A. Kadyk,[5] L. T. Kerth,[5] Yu. G. Kolomensky,[5] G. Kukartsev,[5] G. Lynch,[5] I. L. Osipenkov,[5] M. T. Ronan,[5,*] K. Tackmann,[5] T. Tanabe,[5] W. A. Wenzel,[5] C. M. Hawkes,[6] N. Soni,[6] A. T. Watson,[6] H. Koch,[7] T. Schroeder,[7] D. Walker,[8] D. J. Asgeirsson,[9] T. Cuhadar-Donszelmann,[9] B. G. Fulsom,[9] C. Hearty,[9] T. S. Mattison,[9] J. A. McKenna,[9] M. Barrett,[10] A. Khan,[10] M. Saleem,[10] L. Teodorescu,[10] V. E. Blinov,[11] A. D. Bukin,[11] A. R. Buzykaev,[11] V. P. Druzhinin,[11] V. B. Golubev,[11] A. P. Onuchin,[11] S. I. Serednyakov,[11] Yu. I. Skovpen,[11] E. P. Solodov,[11] K. Yu. Todyshev,[11] M. Bondioli,[12] S. Curry,[12] I. Eschrich,[12] D. Kirkby,[12] A. J. Lankford,[12] P. Lund,[12] M. Mandelkern,[12] E. C. Martin,[12] D. P. Stoker,[12] S. Abachi,[13] C. Buchanan,[13] J. W. Gary,[14] F. Liu,[14] O. Long,[14] B. C. Shen,[14,*] G. M. Vitug,[14] Z. Yasin,[14] L. Zhang,[14] H. P. Paar,[15] S. Rahatlou,[15] V. Sharma,[15] C. Campagnari,[16] T. M. Hong,[16] D. Kovalskyi,[16] M. A. Mazur,[16] J. D. Richman,[16] T. W. Beck,[17] A. M. Eisner,[17] C. J. Flacco,[17] C. A. Heusch,[17] J. Kroseberg,[17] W. S. Lockman,[17] T. Schalk,[17] B. A. Schumm,[17] A. Seiden,[17] M. G. Wilson,[17] L. O. Winstrom,[17] E. Chen,[18] C. H. Cheng,[18] D. A. Doll,[18] B. Echenard,[18] F. Fang,[18] D. G. Hitlin,[18] I. Narsky,[18] T. Piatenko,[18] F. C. Porter,[18] R. Andreassen,[19] G. Mancinelli,[19] B. T. Meadows,[19] K. Mishra,[19] M. D. Sokoloff,[19] F. Blanc,[20] P. C. Bloom,[20] W. T. Ford,[20] J. F. Hirschauer,[20] A. Kreisel,[20] M. Nagel,[20] U. Nauenberg,[20] A. Olivas,[20] J. G. Smith,[20] K. A. Ulmer,[20] S. R. Wagner,[20] R. Ayad,[21,†] A. M. Gabareen,[21] A. Soffer,[21,‡] W. H. Toki,[21] R. J. Wilson,[21] D. D. Altenburg,[22] E. Feltresi,[22] A. Hauke,[22] H. Jasper,[22] M. Karbach,[22] J. Merkel,[22] A. Petzold,[22] B. Spaan,[22] K. Wacker,[22] V. Klose,[23] M. J. Kobel,[23] H. M. Lacker,[23] W. F. Mader,[23] R. Nogowski,[23] J. Schubert,[23] K. R. Schubert,[23] R. Schwierz,[23] J. E. Sundermann,[23] A. Volk,[23] D. Bernard,[24] G. R. Bonneaud,[24] E. Latour,[24] Ch. Thiebaux,[24] M. Verderi,[24] P. J. Clark,[25] W. Gradl,[25] S. Playfer,[25] A. I. Robertson,[25] J. E. Watson,[25] M. Andreotti,[26] D. Bettoni,[26] C. Bozzi,[26] R. Calabrese,[26] A. Cecchi,[26] G. Cibinetto,[26] P. Franchini,[26] E. Luppi,[26] M. Negrini,[26] A. Petrella,[26] L. Piemontese,[26] E. Prencipe,[26] V. Santoro,[26] F. Anulli,[27] R. Baldini-Ferroli,[27] A. Calcaterra,[27] R. de Sangro,[27] G. Finocchiaro,[27] S. Pacetti,[27] P. Patteri,[27] I. M. Peruzzi,[27,§] M. Piccolo,[27] M. Rama,[27] A. Zallo,[27] A. Buzzo,[28] R. Contri,[28] M. Lo Vetere,[28] M. M. Macri,[28] M. R. Monge,[28] S. Passaggio,[28] C. Patrignani,[28] E. Robutti,[28] A. Santroni,[28] S. Tosi,[28] K. S. Chaisanguanthum,[29] M. Morii,[29] R. S. Dubitzky,[30] J. Marks,[30] S. Schenk,[30] U. Uwer,[30] D. J. Bard,[31] P. D. Dauncey,[31] J. A. Nash,[31] W. Panduro Vazquez,[31] M. Tibbetts,[31] P. K. Behera,[32] X. Chai,[32] M. J. Charles,[32] U. Mallik,[32] J. Cochran,[33] H. B. Crawley,[33] L. Dong,[33] V. Eyges,[33] W. T. Meyer,[33] S. Prell,[33] E. I. Rosenberg,[33] A. E. Rubin,[33] Y. Y. Gao,[34] A. V. Gritsan,[34] Z. J. Guo,[34] C. K. Lae,[34] A. G. Denig,[35] M. Fritsch,[35] G. Schott,[35] N. Arnaud,[36] J. Béquilleux,[36] A. D'Orazio,[36] M. Davier,[36] J. Firmino da Costa,[36] G. Grosdidier,[36] A. Höcker,[36] V. Lepeltier,[36] F. Le Diberder,[36] A. M. Lutz,[36] S. Pruvot,[36] P. Roudeau,[36] M. H. Schune,[36] J. Serrano,[36] V. Sordini,[36] A. Stocchi,[36] W. F. Wang,[36] G. Wormser,[36] D. J. Lange,[37] D. M. Wright,[37] I. Bingham,[38] J. P. Burke,[38] C. A. Chavez,[38] J. R. Fry,[38] E. Gabathuler,[38] R. Gamet,[38] D. E. Hutchcroft,[38] D. J. Payne,[38] C. Touramanis,[38] A. J. Bevan,[39] K. A. George,[39] F. Di Lodovico,[39] R. Sacco,[39] M. Sigamani,[39] G. Cowan,[40] H. U. Flaecher,[40] D. A. Hopkins,[40] S. Paramesvaran,[40] F. Salvatore,[40] A. C. Wren,[40] D. N. Brown,[41] C. L. Davis,[41] K. E. Alwyn,[42] N. R. Barlow,[42] R. J. Barlow,[42] Y. M. Chia,[42] C. L. Edgar,[42] G. D. Lafferty,[42] T. J. West,[42] J. I. Yi,[42] J. Anderson,[43] C. Chen,[43] A. Jawahery,[43] D. A. Roberts,[43] G. Simi,[43] J. M. Tuggle,[43] C. Dallapiccola,[44] S. S. Hertzbach,[44] X. Li,[44] E. Salvati,[44] S. Saremi,[44] R. Cowan,[45] D. Dujmic,[45] P. H. Fisher,[45] K. Koeneke,[45] G. Sciolla,[45] M. Spitznagel,[45] F. Taylor,[45] R. K. Yamamoto,[45] M. Zhao,[45] S. E. Mclachlin,[46,*] P. M. Patel,[46] S. H. Robertson,[46] A. Lazzaro,[47] V. Lombardo,[47] F. Palombo,[47] J. M. Bauer,[48] L. Cremaldi,[48] V. Eschenburg,[48] R. Godang,[48] R. Kroeger,[48] D. A. Sanders,[48] D. J. Summers,[48] H. W. Zhao,[48] S. Brunet,[49] D. Côté,[49] M. Simard,[49] P. Taras,[49] F. B. Viaud,[49] H. Nicholson,[50] G. De Nardo,[51] L. Lista,[51] D. Monorchio,[51] C. Sciacca,[51] M. A. Baak,[52] G. Raven,[52] H. L. Snoek,[52] C. P. Jessop,[53] K. J. Knoepfel,[53] J. M. LoSecco,[53] G. Benelli,[54] L. A. Corwin,[54] K. Honscheid,[54] H. Kagan,[54] R. Kass,[54] J. P. Morris,[54] A. M. Rahimi,[54] J. J. Regensburger,[54] S. J. Sekula,[54] Q. K. Wong,[54] N. L. Blount,[55] J. Brau,[55] R. Frey,[55] O. Igonkina,[55] J. A. Kolb,[55] M. Lu,[55] R. Rahmat,[55] N. B. Sinev,[55] D. Strom,[55] J. Strube,[55] E. Torrence,[55] G. Castelli,[56] N. Gagliardi,[56] A. Gaz,[56] M. Margoni,[56] M. Morandin,[56] M. Posocco,[56] M. Rotondo,[56] F. Simonetto,[56] R. Stroili,[56] C. Voci,[56] P. del Amo Sanchez,[57] E. Ben-Haim,[57] H. Briand,[57] G. Calderini,[57] J. Chauveau,[57] P. David,[57] L. Del Buono,[57] O. Hamon,[57] Ph. Leruste,[57] J. Malclès,[57] J. Ocariz,[57] A. Perez,[57] J. Prendki,[57] L. Gladney,[58] M. Biasini,[59] R. Covarelli,[59] E. Manoni,[59] C. Angelini,[60] G. Batignani,[60] S. Bettarini,[60] M. Carpinelli,[60,‖] A. Cervelli,[60] F. Forti,[60] M. A. Giorgi,[60]

A. Lusiani,[60] G. Marchiori,[60] M. Morganti,[60] N. Neri,[60] E. Paoloni,[60] G. Rizzo,[60] J. J. Walsh,[60] J. Biesiada,[61] Y. P. Lau,[61] D. Lopes Pegna,[61] C. Lu,[61] J. Olsen,[61] A. J. S. Smith,[61] A. V. Telnov,[61] E. Baracchini,[62] G. Cavoto,[62] D. del Re,[62] E. Di Marco,[62] R. Faccini,[62] F. Ferrarotto,[62] F. Ferroni,[62] M. Gaspero,[62] P. D. Jackson,[62] M. A. Mazzoni,[62] S. Morganti,[62] G. Piredda,[62] F. Polci,[62] F. Renga,[62] C. Voena,[62] M. Ebert,[63] T. Hartmann,[63] H. Schröder,[63] R. Waldi,[63] T. Adye,[64] B. Franek,[64] E. O. Olaiya,[64] W. Roethel,[64] F. F. Wilson,[64] S. Emery,[65] M. Escalier,[65] A. Gaidot,[65] S. F. Ganzhur,[65] G. Hamel de Monchenault,[65] W. Kozanecki,[65] G. Vasseur,[65] Ch. Yèche,[65] M. Zito,[65] X. R. Chen,[66] H. Liu,[66] W. Park,[66] M. V. Purohit,[66] R. M. White,[66] J. R. Wilson,[66] M. T. Allen,[67] D. Aston,[67] R. Bartoldus,[67] P. Bechtle,[67] J. F. Benitez,[67] R. Cenci,[67] J. P. Coleman,[67] M. R. Convery,[67] J. C. Dingfelder,[67] J. Dorfan,[67] G. P. Dubois-Felsmann,[67] W. Dunwoodie,[67] R. C. Field,[67] T. Glanzman,[67] S. J. Gowdy,[67] M. T. Graham,[67] P. Grenier,[67] C. Hast,[67] W. R. Innes,[67] J. Kaminski,[67] M. H. Kelsey,[67] H. Kim,[67] P. Kim,[67] M. L. Kocian,[67] D. W. G. S. Leith,[67] S. Li,[67] B. Lindquist,[67] S. Luitz,[67] V. Luth,[67] H. L. Lynch,[67] D. B. MacFarlane,[67] H. Marsiske,[67] R. Messner,[67] D. R. Muller,[67] H. Neal,[67] S. Nelson,[67] C. P. O'Grady,[67] I. Ofte,[67] A. Perazzo,[67] M. Perl,[67] B. N. Ratcliff,[67] A. Roodman,[67] A. A. Salnikov,[67] R. H. Schindler,[67] J. Schwiening,[67] A. Snyder,[67] D. Su,[67] M. K. Sullivan,[67] K. Suzuki,[67] S. K. Swain,[67] J. M. Thompson,[67] J. Va'vra,[67] A. P. Wagner,[67] M. Weaver,[67] W. J. Wisniewski,[67] M. Wittgen,[67] D. H. Wright,[67] H. W. Wulsin,[67] A. K. Yarritu,[67] K. Yi,[67] C. C. Young,[67] V. Ziegler,[67] P. R. Burchat,[68] A. J. Edwards,[68] S. A. Majewski,[68] T. S. Miyashita,[68] B. A. Petersen,[68] L. Wilden,[68] S. Ahmed,[69] M. S. Alam,[69] R. Bula,[69] J. A. Ernst,[69] B. Pan,[69] M. A. Saeed,[69] S. B. Zain,[69] S. M. Spanier,[70] B. J. Wogsland,[70] R. Eckmann,[71] J. L. Ritchie,[71] A. M. Ruland,[71] C. J. Schilling,[71] R. F. Schwitters,[71] J. M. Izen,[72] X. C. Lou,[72] S. Ye,[72] F. Bianchi,[73] D. Gamba,[73] M. Pelliccioni,[73] M. Bomben,[74] L. Bosisio,[74] C. Cartaro,[74] F. Cossutti,[74] G. Della Ricca,[74] L. Lanceri,[74] L. Vitale,[74] V. Azzolini,[75] N. Lopez-March,[75] F. Martinez-Vidal,[75] D. A. Milanes,[75] A. Oyanguren,[75] J. Albert,[76] Sw. Banerjee,[76] B. Bhuyan,[76] K. Hamano,[76] R. Kowalewski,[76] I. M. Nugent,[76] J. M. Roney,[76] R. J. Sobie,[76] T. J. Gershon,[77] P. F. Harrison,[77] J. Ilic,[77] T. E. Latham,[77] G. B. Mohanty,[77] H. R. Band,[78] X. Chen,[78] S. Dasu,[78] K. T. Flood,[78] P. E. Kutter,[78] Y. Pan,[78] M. Pierini,[78] R. Prepost,[78] C. O. Vuosalo,[78] and S. L. Wu[78]

(*BABAR* Collaboration)

[1]*Laboratoire de Physique des Particules, IN2P3/CNRS et Université de Savoie, F-74941 Annecy-Le-Vieux, France*
[2]*Universitat de Barcelona, Facultat de Fisica, Departament ECM, E-08028 Barcelona, Spain*
[3]*Università di Bari, Dipartimento di Fisica and INFN, I-70126 Bari, Italy*
[4]*University of Bergen, Institute of Physics, N-5007 Bergen, Norway*
[5]*Lawrence Berkeley National Laboratory and University of California, Berkeley, California 94720, USA*
[6]*University of Birmingham, Birmingham, B15 2TT, United Kingdom*
[7]*Ruhr Universität Bochum, Institut für Experimentalphysik 1, D-44780 Bochum, Germany*
[8]*University of Bristol, Bristol BS8 1TL, United Kingdom*
[9]*University of British Columbia, Vancouver, British Columbia, Canada V6T 1Z1*
[10]*Brunel University, Uxbridge, Middlesex UB8 3PH, United Kingdom*
[11]*Budker Institute of Nuclear Physics, Novosibirsk 630090, Russia*
[12]*University of California at Irvine, Irvine, California 92697, USA*
[13]*University of California at Los Angeles, Los Angeles, California 90024, USA*
[14]*University of California at Riverside, Riverside, California 92521, USA*
[15]*University of California at San Diego, La Jolla, California 92093, USA*
[16]*University of California at Santa Barbara, Santa Barbara, California 93106, USA*
[17]*University of California at Santa Cruz, Institute for Particle Physics, Santa Cruz, California 95064, USA*
[18]*California Institute of Technology, Pasadena, California 91125, USA*
[19]*University of Cincinnati, Cincinnati, Ohio 45221, USA*
[20]*University of Colorado, Boulder, Colorado 80309, USA*
[21]*Colorado State University, Fort Collins, Colorado 80523, USA*
[22]*Universität Dortmund, Institut für Physik, D-44221 Dortmund, Germany*
[23]*Technische Universität Dresden, Institut für Kernund Teilchenphysik, D-01062 Dresden, Germany*
[24]*Laboratoire Leprince-Ringuet, CNRS/IN2P3, Ecole Polytechnique, F-91128 Palaiseau, France*
[25]*University of Edinburgh, Edinburgh EH9 3JZ, United Kingdom*
[26]*Università di Ferrara, Dipartimento di Fisica and INFN, I-44100 Ferrara, Italy*
[27]*Laboratori Nazionali di Frascati dell'INFN, I-00044 Frascati, Italy*
[28]*Università di Genova, Dipartimento di Fisica and INFN, I-16146 Genova, Italy*
[29]*Harvard University, Cambridge, Massachusetts 02138, USA*
[30]*Universität Heidelberg, Physikalisches Institut, Philosophenweg 12, D-69120 Heidelberg, Germany*
[31]*Imperial College London, London, SW7 2AZ, United Kingdom*
[32]*University of Iowa, Iowa City, Iowa 52242, USA*

[33]*Iowa State University, Ames, Iowa 50011-3160, USA*
[34]*Johns Hopkins University, Baltimore, Maryland 21218, USA*
[35]*Universität Karlsruhe, Institut für Experimentelle Kernphysik, D-76021 Karlsruhe, Germany*
[36]*Laboratoire de l'Accélérateur Linéaire, IN2P3/CNRS et Université Paris-Sud 11, Centre Scientifique d'Orsay, B. P. 34, F-91898 ORSAY Cedex, France*
[37]*Lawrence Livermore National Laboratory, Livermore, California 94550, USA*
[38]*University of Liverpool, Liverpool L69 7ZE, United Kingdom*
[39]*Queen Mary, University of London, E1 4NS, United Kingdom*
[40]*University of London, Royal Holloway and Bedford New College, Egham, Surrey TW20 0EX, United Kingdom*
[41]*University of Louisville, Louisville, Kentucky 40292, USA*
[42]*University of Manchester, Manchester M13 9PL, United Kingdom*
[43]*University of Maryland, College Park, Maryland 20742, USA*
[44]*University of Massachusetts, Amherst, Massachusetts 01003, USA*
[45]*Massachusetts Institute of Technology, Laboratory for Nuclear Science, Cambridge, Massachusetts 02139, USA*
[46]*McGill University, Montréal, Québec, Canada H3A 2T8*
[47]*Università di Milano, Dipartimento di Fisica and INFN, I-20133 Milano, Italy*
[48]*University of Mississippi, University, Mississippi 38677, USA*
[49]*Université de Montréal, Physique des Particules, Montréal, Québec, Canada H3C 3J7*
[50]*Mount Holyoke College, South Hadley, Massachusetts 01075, USA*
[51]*Università di Napoli Federico II, Dipartimento di Scienze Fisiche and INFN, I-80126, Napoli, Italy*
[52]*NIKHEF, National Institute for Nuclear Physics and High Energy Physics, NL-1009 DB Amsterdam, The Netherlands*
[53]*University of Notre Dame, Notre Dame, Indiana 46556, USA*
[54]*Ohio State University, Columbus, Ohio 43210, USA*
[55]*University of Oregon, Eugene, Oregon 97403, USA*
[56]*Università di Padova, Dipartimento di Fisica and INFN, I-35131 Padova, Italy*
[57]*Laboratoire de Physique Nucléaire et de Hautes Energies, IN2P3/CNRS, Université Pierre et Marie Curie-Paris6, Université Denis Diderot-Paris7, F-75252 Paris, France*
[58]*University of Pennsylvania, Philadelphia, Pennsylvania 19104, USA*
[59]*Università di Perugia, Dipartimento di Fisica and INFN, I-06100 Perugia, Italy*
[60]*Università di Pisa, Dipartimento di Fisica, Scuola Normale Superiore and INFN, I-56127 Pisa, Italy*
[61]*Princeton University, Princeton, New Jersey 08544, USA*
[62]*Università di Roma La Sapienza, Dipartimento di Fisica and INFN, I-00185 Roma, Italy*
[63]*Universität Rostock, D-18051 Rostock, Germany*
[64]*Rutherford Appleton Laboratory, Chilton, Didcot, Oxon, OX11 0QX, United Kingdom*
[65]*DSM/Dapnia, CEA/Saclay, F-91191 Gif-sur-Yvette, France*
[66]*University of South Carolina, Columbia, South Carolina 29208, USA*
[67]*Stanford Linear Accelerator Center, Stanford, California 94309, USA*
[68]*Stanford University, Stanford, California 94305-4060, USA*
[69]*State University of New York, Albany, New York 12222, USA*
[70]*University of Tennessee, Knoxville, Tennessee 37996, USA*
[71]*University of Texas at Austin, Austin, Texas 78712, USA*
[72]*University of Texas at Dallas, Richardson, Texas 75083, USA*
[73]*Università di Torino, Dipartimento di Fisica Sperimentale and INFN, I-10125 Torino, Italy*
[74]*Università di Trieste, Dipartimento di Fisica and INFN, I-34127 Trieste, Italy*
[75]*IFIC, Universitat de Valencia-CSIC, E-46071 Valencia, Spain*
[76]*University of Victoria, Victoria, British Columbia, Canada V8W 3P6*
[77]*Department of Physics, University of Warwick, Coventry CV4 7AL, United Kingdom*
[78]*University of Wisconsin, Madison, Wisconsin 53706, USA*
(Received 15 May 2008; published 15 April 2009)

We present constraints on the angle γ of the unitarity triangle with a Dalitz analysis of neutral D decays to $K_S\pi^+\pi^-$ from the processes $B^0 \to \bar{D}^0 K^{*0}$ ($\bar{B}^0 \to D^0 \bar{K}^{*0}$) and $B^0 \to D^0 K^{*0}$ ($\bar{B}^0 \to \bar{D}^0 \bar{K}^{*0}$) with $K^{*0} \to K^+\pi^-$ ($\bar{K}^{*0} \to K^-\pi^+$). Using a sample of 371×10^6 $B\bar{B}$ pairs collected with the *BABAR* detector at PEP-II, we constrain the angle γ as a function of r_S, the magnitude of the average ratio between $b \to u$ and $b \to c$ amplitudes.

*Deceased.
†Now at Temple University, Philadelphia, PA 19122, USA.
‡Now at Tel Aviv University, Tel Aviv, 69978, Israel.
§Also with Università di Perugia, Dipartimento di Fisica, Perugia, Italy.
‖Also with Universitá di Sassari, Sassari, Italy.

DOI: 10.1103/PhysRevD.79.072003 PACS numbers: 13.25.Hw, 14.40.Nd

I. INTRODUCTION

Various methods have been proposed to determine the unitarity triangle angle γ [1–3] of the Cabibbo-Kobayashi-Maskawa (CKM) quark mixing matrix [4] using $B^- \to \tilde{D}^{(*)0}K^{(*)-}$ decays, where the symbol $\tilde{D}^{(*)0}$ indicates either a $D^{(*)0}$ or a $\bar{D}^{(*)0}$ meson. A B^- can decay into a $\tilde{D}^{(*)0}K^{(*)-}$ final state via a $b \to c$ or a $b \to u$ mediated process and CP violation can be detected when the $D^{(*)0}$ and the $\bar{D}^{(*)0}$ decay to the same final state. These processes are thus sensitive to $\gamma = \arg\{-V_{ub}^* V_{ud}/V_{cb}^* V_{cd}\}$. The present determination of γ comes from the combination of several results obtained with the different methods. In particular, the Dalitz technique [3], when used to analyze $B^- \to \tilde{D}^{(*)0}K^{(*)-}$ decays, is very powerful, resulting in an error on γ of about 24° and 13° for the *BABAR* and Belle analyses, respectively, ([5,6]). These results are obtained from the simultaneous exploitation of the three decays of the charged B mesons ($B^- \to \tilde{D}^0 K^-$, $\tilde{D}^{*0}K^-$, and $\tilde{D}^0 K^{*-}$) and, in the case of *BABAR*, from the study of two final states for the neutral D mesons ($K_S\pi^+\pi^-$ and $K_S K^+ K^-$).

In this paper we present the first measurement of the angle γ using neutral B meson decays. We reconstruct $B^0 \to \tilde{D}^0 K^{*0}$, with $K^{*0} \to K^+\pi^-$ (charge conjugate processes are assumed throughout the paper and K^{*0} refers to $K^*(892)^0$), where the flavor of the B meson is identified by the kaon electric charge. Neutral D mesons are reconstructed in the $K_S\pi^+\pi^-$ decay mode and are analyzed with the Dalitz technique [3]. The final states we reconstruct can be reached through $b \to c$ and $b \to u$ processes with the diagrams shown in Fig. 1. The correlation within the flavor of the neutral D meson and the charge of the kaon in the final state allows for discriminating between events arising from $b \to c$ and $b \to u$ transitions. In particular it is useful for the following discussion to stress that $\bar{b} \to \bar{u}$ (B^0) transitions lead to $D^0 K^+\pi^-$ final states and $b \to u$ ($\bar{B}^0$) transitions lead to $\bar{D}^0 K^-\pi^+$ final states.

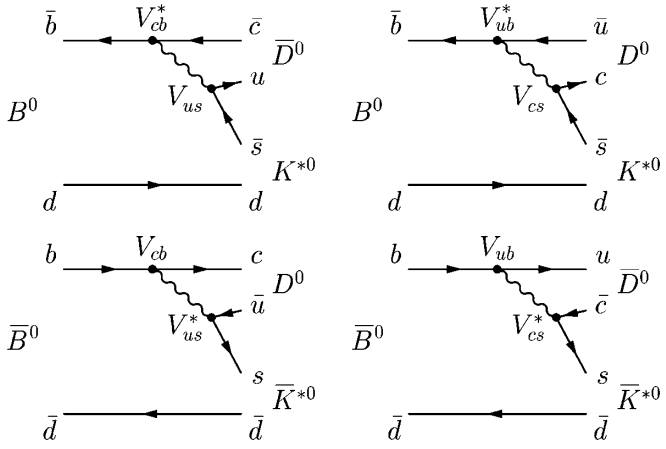

FIG. 1. Feynman diagrams for the decays $B^0 \to \bar{D}^0 K^{*0}$ (upper left, $\bar{b} \to \bar{c}$ transition), $B^0 \to D^0 K^{*0}$ (upper right, $\bar{b} \to \bar{u}$ transition), $\bar{B}^0 \to D^0 \bar{K}^{*0}$ (lower left, $b \to c$ transition), and $\bar{B}^0 \to \bar{D}^0 \bar{K}^{*0}$ (lower right, $b \to u$ transition). A K^{*0} is a decay product of a B^0 while a $\bar{K}^{*0}$ results from a $\bar{B}^0$ decay.

When analyzing $B^0 \to \tilde{D}^0 K^{*0}$ decays, the natural width of the K^{*0} (50 MeV/c^2) has to be considered. In the K^{*0} mass region, amplitudes for decays to higher-mass $K\pi$ resonances interfere with the signal decay amplitude and with each other. For this analysis we use effective variables, introduced in Ref. [7], obtained by integrating over a region of the $B^0 \to \tilde{D}^0 K^+\pi^-$ Dalitz plot corresponding to the K^{*0}. For this purpose we introduce the quantities r_S, k, and δ_S defined as

$$r_S^2 \equiv \frac{\Gamma(B^0 \to D^0 K^+\pi^-)}{\Gamma(B^0 \to \bar{D}^0 K^+\pi^-)} = \frac{\int dp A_u^2(p)}{\int dp A_c^2(p)}, \tag{1}$$

$$k e^{i\delta_S} \equiv \frac{\int dp A_c(p) A_u(p) e^{i\delta(p)}}{\sqrt{\int dp A_c^2(p) \int dp A_u^2(p)}}, \tag{2}$$

where $0 \le k \le 1$ and $\delta_S \in [0, 2\pi]$. The amplitudes for the $b \to c$ and $b \to u$ transitions, $A_c(p)$ and $A_u(p)$, are real and positive and $\delta(p)$ is the relative strong phase. The variable p indicates the position in the $\tilde{D}^0 K^+\pi^-$ Dalitz plot. In case of a two-body B decay, r_S and δ_S become $r_B = |A_u|/|A_c|$ and δ_B (the strong phase difference between A_u and A_c) and $k = 1$. Because of CKM factors and the fact that both diagrams, for the neutral B decays we consider, are color-suppressed, the average amplitude ratio r_S in $B^0 \to \tilde{D}^0 K^{*0}$ is expected to be in the range [0.3, 0.5], larger than the analogous ratio for charged $B^\pm \to \tilde{D}^0 K^\pm$ decays (which is of the order of 10% [8,9]). An earlier measurement sets an upper limit $r_S < 0.4$ at 90% probability [10]. A phenomenological approach [11] proposed to evaluate r_B in the $B^0 \to \tilde{D}^0 K^0$ system gives $r_B = 0.27 \pm 0.18$.

II. EVENT RECONSTRUCTION AND SELECTION

The analysis presented in this paper uses a data sample of 371×10^6 $B\bar{B}$ pairs collected with the *BABAR* detector at the PEP-II storage ring. Approximately 10% of the collected data (35 fb^{-1}) have a center-of-mass (CM) energy 40 MeV below the $\Upsilon(4S)$ resonance. These "off-resonance" data are used to study backgrounds from continuum events, $e^+e^- \to q\bar{q}$ ($q = u$, d, s, or c).

The *BABAR* detector is described elsewhere [12]. Charged-particle tracking is provided by a five-layer silicon vertex tracker (SVT) and a 40-layer drift chamber (DCH). In addition to providing precise position information for tracking, the SVT and DCH also measure the specific ionization (dE/dx), which is used for particle identification of low-momentum charged particles. At higher momenta ($p > 0.7$ GeV/c) pions and kaons are

identified by Cherenkov radiation detected in a ring-imaging device (DIRC). The position and energy of photons are measured with an electromagnetic calorimeter (EMC) consisting of 6580 thallium-doped CsI crystals. These systems are mounted inside a 1.5 T solenoidal superconducting magnet.

We reconstruct $B^0 \to \tilde{D}^0 K^{*0}$ events with $K^{*0} \to K^+\pi^-$ and $\tilde{D}^0 \to K_S\pi^+\pi^-$. The event selection, described below, is developed from studies of off-resonance data and events simulated with Monte Carlo techniques (MC). The K_S is reconstructed from pairs of oppositely charged pions with invariant mass within 7 MeV/c^2 of the nominal K_S mass [13], corresponding to 2.8 standard deviations of the mass distribution for signal events. We also require that $\cos\alpha_{K_S}(\tilde{D}^0) > 0.997$, where $\alpha_{K_S}(\tilde{D}^0)$ is the angle between the K_S line of flight (line between the $\tilde{D}^0$ and the K_S decay points) and the K_S momentum (measured from the two pion momenta). Neutral D candidates are selected by combining K_S candidates with two oppositely charged pion candidates and requiring the $\tilde{D}^0$ invariant mass to be within 11 MeV/c^2 of its nominal mass [13], corresponding to 1.8 standard deviations of the mass distribution for signal events. The K_S and the two pions used to reconstruct the $\tilde{D}^0$ are constrained to originate from a common vertex. The charged kaon is required to satisfy kaon identification criteria, which are based on Cherenkov angle and dE/dx measurements and are typically 85% efficient, depending on momentum and polar angle. Misidentification rates are at the 2% level. The tracks used to reconstruct the K^{*0} are constrained to originate from a common vertex and their invariant mass is required to lie within 48 MeV/c^2 of the nominal K^{*0} mass [13]. We define $\theta_{\rm Hel}$ as the angle between the direction of flight of the charged K in the K^{*0} rest frame with respect to the direction of flight of the K^{*0} in the B rest frame. The distribution of $\cos\theta_{\rm Hel}$ is expected to be proportional to $\cos^2\theta_{\rm Hel}$ for signal events, due to angular momentum conservation, and flat for background events. We require $|\cos\theta_{\rm Hel}| > 0.3$. The cuts on the K^{*0} mass and on $|\cos\theta_{\rm Hel}|$ have been optimized maximizing the function $S/\sqrt{S+B}$, where S and B are the expected numbers of signal and background events, respectively, based on MC studies. The B^0 candidates are reconstructed by combining one $\tilde{D}^0$ and one K^{*0} candidate, constraining them to originate from a common vertex with a probability greater than 0.001. The distribution of the cosine of the B polar angle with respect to the beam axis in the e^+e^- CM frame, $\cos\theta_B$, is expected to be proportional to $1-\cos^2\theta_B$. We require $|\cos\theta_B| < 0.9$.

We measure two almost independent kinematic variables: the beam-energy substituted mass $m_{\rm ES} \equiv \sqrt{(E_0^{*2}/2 + \vec{p}_0\cdot\vec{p}_B)^2/E_0^2 - p_B^2}$, and the energy difference $\Delta E \equiv E_B^* - E_0^*/2$, where E and p are energy and momentum, the subscripts B and 0 refer to the candidate B and to the e^+e^- system, respectively, and the asterisk denotes the e^+e^- CM frame. For signal events, $m_{\rm ES}$ is centered around the B mass with a resolution of about 2.5 MeV/c^2, and ΔE is centered at zero with a resolution of 12.5 MeV. The B candidates are required to have ΔE in the range $[-0.025, 0.025]$ GeV. As it will be explained in Sec. IV, the variable $m_{\rm ES}$ is used in the fit procedure for the signal extraction. For this reason, the requirements on it are quite loose: $m_{\rm ES} \in [5.20, 5.29]$ GeV/c^2. The region 5.20 GeV/$c^2 < m_{\rm ES} <$ 5.27 GeV/c^2, free from any signal contribution, is exploited in the fit to characterize the background directly on data. The proper time interval Δt between the two B decays is calculated from the measured separation, Δz, between the decay points of the reconstructed B ($B_{\rm rec}$) and the other B ($B_{\rm oth}$) along the beam direction. We accept events with calculated Δt uncertainty less than 2.5 ps and $|\Delta t| < 20$ ps. In less than 1% of the cases, multiple candidates are present in the same event and we choose the one with reconstructed $\tilde{D}^0$ mass closest to the nominal mass [13]. In the case of two B candidates reconstructed from the same $\tilde{D}^0$, we choose the candidate with the largest value of $|\cos\theta_{\rm Hel}|$. The overall reconstruction and selection efficiency for signal, evaluated on MC, is $(10.8 \pm 0.5)\%$.

III. BACKGROUND CHARACTERIZATION

After applying the selection criteria described above, the background is composed of continuum events ($e^+e^- \to q\bar{q}$, $q = u, d, s, c$) and $\Upsilon(4S) \to B\bar{B}$ events ("$B\bar{B}$", in the following). To discriminate against the continuum background events (the dominant background component), which, in contrast to $B\bar{B}$ events, have a jetlike shape, we use a Fisher discriminant $\mathcal{F}$ [14]. The discriminant $\mathcal{F}$ is a linear combination of three variables: $\cos\theta_{\rm thrust}$, the cosine of the angle between the B thrust axis and the thrust axis of the rest of the event; $L_0 = \sum_i p_i$; and $L_2 = \sum_i p_i |\cos\theta_i|^2$. Here, p_i is the momentum and θ_i is the angle with respect to the thrust axis of the B candidate. The index i runs over all the reconstructed tracks and energy deposits in the calorimeter not associated with a track. The tracks and energy deposits used to reconstruct the B are excluded from these sums. All these variables are calculated in the e^+e^- CM frame. The coefficients of the Fisher discriminant, chosen to maximize the separation between signal and continuum background, are determined using signal MC events and off-resonance data. A cut on this variable with 85% efficiency on simulated signal events would reject about 80% of continuum background events, as estimated on off-resonance data. We choose not to cut on the Fisher discriminant, as we will use this variable in the fit procedure to extract the signal. The variable Δt gives further discrimination between signal and continuum events. For events in which the B meson has been correctly reconstructed, the Δt distribution is the convolution of a decreasing exponential function e^{-t/τ_B} (with τ_B equal to the B lifetime) with the resolution on Δz from the detector reconstruction. The distribution is then wider than in the

case of continuum events, in which just the resolution effect is observed.

The $B_{\rm rec}$ decay point is the common vertex of the B decay products. The $B_{\rm oth}$ decay point is obtained using tracks which do not belong to $B_{\rm rec}$ and imposing constraints from the $B_{\rm rec}$ momentum and the beam-spot location.

Background events for which the reconstructed K_S, π^+, and π^- come from a real $\tilde{D}^0$ ("true D^0" in the following) are treated separately because of their distribution over the $\tilde{D}^0$ Dalitz plane. A fit to the $K_S\pi^+\pi^-$ invariant mass distribution for events in the $m_{\rm ES}$ sideband ($m_{\rm ES} < 5.27\ {\rm GeV}/c^2$) has been performed on data to obtain the fraction of true D^0 equal to 0.289 ± 0.028. This value is in agreement with that determined from simulated $B\bar{B}$ and continuum background samples.

Background events with final states containing $D^0h^+\pi^-$ or $\bar{D}^0h^-\pi^+$, where $h^\pm$ is a candidate $K^\pm$ and $\tilde{D}^0 \to K_S\pi^+\pi^-$, can mimic $b\to u$ mediated signal events (see Fig. 1). The fraction of these events (relative to the number of true D^0 events), defined as $R_{b\to u} = [N(D^0h^+\pi^-) + N(\bar{D}^0h^-\pi^+)]/[N(D^0h^+\pi^-) + N(D^0h^-\pi^+) + N(\bar{D}^0h^+\pi^-) + N(\bar{D}^0h^-\pi^+)]$, has been found to be 0.88 ± 0.02 and 0.45 ± 0.12 in $B\bar{B}$ and continuum MC events, respectively.

Studies have been performed on B decays, which have the same final state reconstructed particles as the signal decay (so-called peaking background). From MC studies, we identify three possible background sources of this kind: $B^0 \to \tilde{D}^0K^{*0}$ ($K^{*0} \to K^+\pi^-$, $\tilde{D}^0 \to \pi^+\pi^-\pi^+\pi^-$), $B^0 \to \tilde{D}^0\rho^0$ ($\rho^0 \to \pi^+\pi^-$, $\tilde{D}^0 \to K_S\pi^+\pi^-$, where ρ^0 is reconstructed as a K^{*0} with a misidentified pion) and charmless events of the kind $B^0 \to K^{*0}K_SK_S$. To precisely evaluate the selection efficiency for $\tilde{D}^0\rho^0$ and $\tilde{D}^0K^{*0}$ with $\tilde{D}^0 \to \pi^+\pi^-\pi^+\pi^-$, dedicated MC samples have been generated, resulting in $(0.04 \pm 0.02)\%$ or $(0.18 \pm 0.04)\%$, respectively. With these efficiencies, we expect to select about 0.9 $\tilde{D}^0\rho^0$ events and 0.1 $\tilde{D}^0 \to 4\pi$ events in 371×10^6 $B\bar{B}$ pairs. In the latter case the requirement on α_{K_S} rejects most of the background, while for $\tilde{D}^0\rho^0$ the cuts on ΔE and the particle identification of the $K^\pm$ are the most effective. The number of charmless background events has been evaluated on data from the D^0 mass sidebands, namely $M_{K_S\pi^+\pi^-}$ in the range [1.810, 1.839] or $[1.889, 1.920]\,{\rm GeV}/c^2$; we obtain $N_{\rm peak} = -5 \pm 7$ events, consistent with 0. Hence we assume these background sources can be neglected in our signal extraction procedure; the effects of this assumption are taken into account in the evaluation of the systematic uncertainties. The remaining $B\bar{B}$ background is combinatorial.

IV. LIKELIHOOD FIT AND MEASURED YIELD

We perform an unbinned extended maximum likelihood fit to the variables $m_{\rm ES}$, $\mathcal{F}$, and Δt, in order to extract the signal, continuum and $B\bar{B}$ background yields, probability density function (PDF) shape parameters, and CP parameters. We write the likelihood as

$$\mathcal{L} = \frac{e^{-\eta}\eta^N}{N!}\prod_\alpha\prod_{i=1}^{N_\alpha}\mathcal{P}^\alpha(i), \tag{3}$$

where $\mathcal{P}^\alpha(i)$ and N_α are the PDF for event i and the total number of events for component α (signal, $B\bar{B}$ background, continuum background). Here N is the total number of selected events and η is the expected value for the total number of events, according to Poisson statistics. The PDF is the product of a "yield" PDF $\mathcal{P}^\alpha(m_{\rm ES})\mathcal{P}^\alpha(\mathcal{F})\times\mathcal{P}^\alpha(\Delta t)$ (written as a product of one-dimensional PDFs since $m_{\rm ES}$, $\mathcal{F}$,and Δt are not correlated) and of the D^0 Dalitz plot dependent part: $\mathcal{P}^\alpha(m_+^2, m_-^2)$ (where $m_+^2 = m^2_{K_S\pi^+}$ and $m_-^2 = m^2_{K_S\pi^-}$).

The $m_{\rm ES}$ distribution is parametrized by a Gaussian function for the signal and by an Argus function [15] that is different for continuum and $B\bar{B}$ backgrounds. The $\mathcal{F}$ distribution is parametrized using an asymmetric Gaussian distribution for the signal and $B\bar{B}$ background and the sum of two Gaussian distributions for the continuum background. For the signal, $|\Delta t|$ is parametrized with an exponential decay PDF $e^{-t/\tau}$ in which $\tau = \tau_{B^0}$ [13], convolved with a resolution function that is a sum of three Gaussians [16]. A similar parametrization is used for the backgrounds using exponential distributions with effective lifetimes.

The continuum background parameters are obtained from off-resonance data, while the $B\bar{B}$ parameters are taken from MC. The fractions of true D^0 and the ratios $R_{b\to u}$ in the backgrounds are fixed in the fit to the values obtained on data and MC, respectively.

Using the effective parameters defined in Eqs. (1) and (2), the partial decay rate for events with true D^0 can be written as follows:

$$\begin{aligned}\Gamma(B^0 \to D[K_S\pi^-\pi^+]K^+\pi^-) \propto\ & |\mathcal{P}_-^{\rm Sig}|^2 + r_S^2|\mathcal{P}_+^{\rm Sig}|^2 \\ & + 2kr_S|\mathcal{P}_-^{\rm Sig}||\mathcal{P}_+^{\rm Sig}| \\ & \times\cos(\delta_S + \delta_{D-} - \gamma),\end{aligned} \tag{4}$$

$$\begin{aligned}\Gamma(\bar{B}^0 \to D[K_S\pi^-\pi^+]K^-\pi^+) \propto\ & |\mathcal{P}_+^{\rm Sig}|^2 + r_S^2|\mathcal{P}_-^{\rm Sig}|^2 \\ & + 2kr_S|\mathcal{P}_+^{\rm Sig}||\mathcal{P}_-^{\rm Sig}| \\ & \times\cos(\delta_S + \delta_{D+} + \gamma),\end{aligned} \tag{5}$$

where $\mathcal{P}_+^{\rm Sig} \equiv \mathcal{P}^{\rm Sig}(m_+^2, m_-^2)$, $\mathcal{P}_-^{\rm Sig} \equiv \mathcal{P}^{\rm Sig}(m_-^2, m_+^2)$, and where $\delta_{D+} \equiv \delta_D(m_+^2, m_-^2)$ is the strong phase difference between $\mathcal{P}_+^{\rm Sig}$ and $\mathcal{P}_-^{\rm Sig}$ and $\delta_{D-} \equiv \delta_D(m_-^2, m_+^2)$ is the strong phase difference between $\mathcal{P}_-^{\rm Sig}$ and $\mathcal{P}_+^{\rm Sig}$.

For the resonance structure of the $D^0 \to K_S\pi^+\pi^-$ decay amplitude, $\mathcal{P}_+^{\rm Sig}$, we use the same model as documented in [5]. This is determined on a large data sample (about 487 000 events, with 97.7% purity) from a Dalitz plot analysis of D^0 mesons from $D^{*+} \to D^0\pi^+$ decays produced in $e^+e^- \to c\bar{c}$ events. The decay amplitude is parametrized, using an isobar model, with the sum of the contributions of ten two-body decay modes with intermediate resonances. In addition, the K-matrix approach [17] is used to describe the S-wave component of the $\pi^+\pi^-$ system, which is characterized by the overlap of broad resonances. The systematic effects of the assumptions made on the model used to describe the decay amplitude of neutral D mesons into $K_S\pi^+\pi^-$ final states are evaluated, as it will be described. To account for possible selection efficiency variations across the Dalitz plane, the efficiency is parametrized with a polynomial function whose parameters are evaluated on MC. This function is convoluted with the Dalitz distribution $\mathcal{P}_+^{\rm Sig}$. The distribution over the Dalitz plot for events with no true D^0 is parametrized with a polynomial function whose parameters are evaluated on MC.

Following Ref. [18], we have performed a study to evaluate the possible variations of r_S and k over the $B^0 \to \tilde{D}^0K^+\pi^-$ Dalitz plot. For this purpose we have built a B^0 Dalitz model suggested by recent measurements [11,19], including $K^*(892)^0$, $K_0^*(1430)^0$, $K_2^*(1430)^0$, $K^*(1680)^0$, $D_{s2}(2573)^{\pm}$, $D_2^*(2460)^{\pm}$, and $D_0^*(2308)^{\pm}$ contributions. We have considered the region within 48 MeV/c^2 of the nominal mass of the $K^*(892)^0$ resonance and obtained the distribution of r_S and k by randomly varying all the strong phases ($[0, 2\pi]$) and the amplitudes (within [0.7, 1.3] of their nominal value). The ratio between $b \to u$ and $b \to c$ amplitudes for each resonance has been fixed to 0.4. In the $K^*(892)^0$ mass region, we find that r_S varies between 0.30 and 0.45 depending upon the values of the contributing phases and of the amplitudes. The distribution of k is quite narrow, centered at 0.95 with a rms of 0.02. The study has been repeated varying the ratio between $b \to u$ and $b \to c$ amplitudes between 0.2 and 0.6, leading to very similar results. For these reasons the value of k has been fixed to 0.95 and a variation of 0.03 has been considered for the systematic uncertainties evaluation. On the contrary, r_S will be extracted from data.

We perform the fit for the yields on data extracting the number of events for signal, continuum, and $B\bar{B}$, as well as the slope of the Argus function for the $B\bar{B}$ background. The fitting procedure has been validated using simulated events. We find no bias on the number of fitted events for any of the components. The fit projection for $m_{\rm ES}$ is shown in Fig. 2. We find 39 ± 9 signal, 231 ± 28 $B\bar{B}$, and 1772 ± 48 continuum events. In Fig. 2 we also show, for illustration purposes, the fit projection for $m_{\rm ES}$, after a cut on $\mathcal{F} > 0.4$ is applied, to visually enhance the signal. Such a cut has an approximate efficiency of 75% on signal, while it rejects 90% of the continuum background.

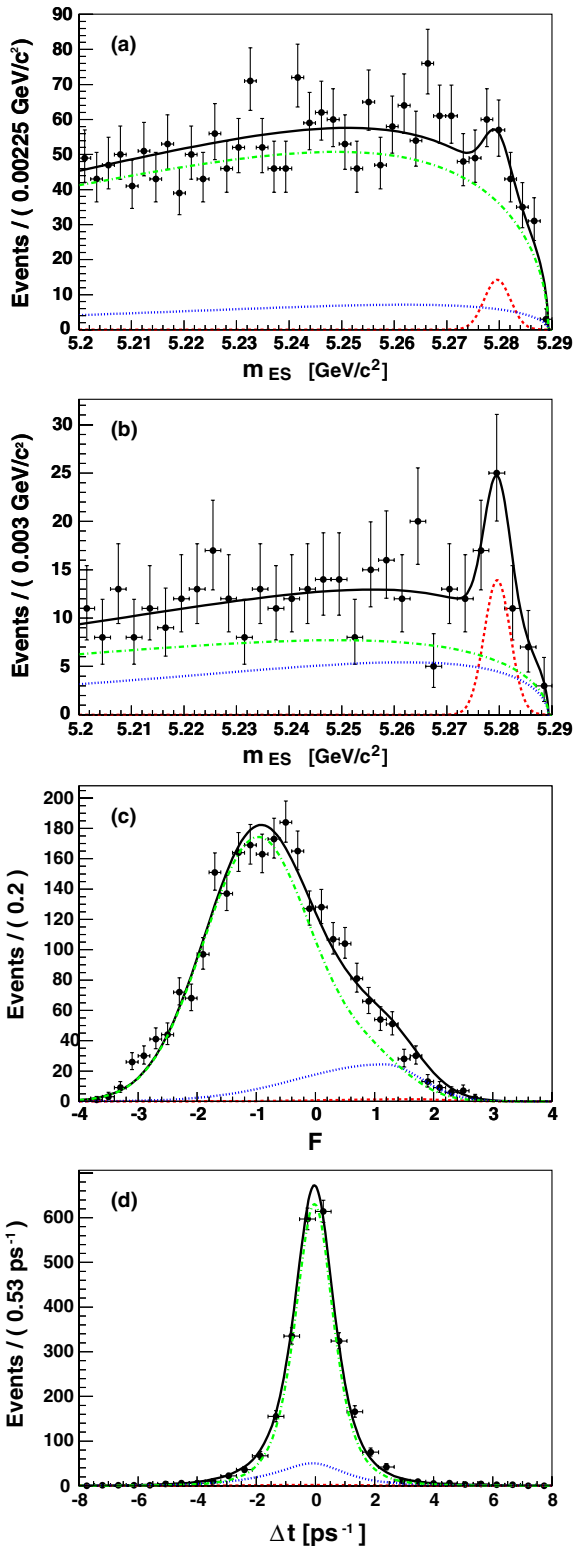

FIG. 2 (color online). $m_{\rm ES}$ projection from the fit (a). The data are indicated with dots and error bars and the different fit components are shown: signal (dashed), $B\bar{B}$ (dotted), and continuum (dot-dashed). With a different binning (b), $m_{\rm ES}$ projection after a cut on $\mathcal{F} > 0.4$ is applied, to visually enhance the signal. $\mathcal{F}$ and Δt projection from the fit (c), (d).

V. DETERMINATION OF γ

From the fit to the data we obtain a three-dimensional likelihood $\mathcal{L}$ for γ, δ_S, and r_S which includes only statistical uncertainties. We convolve this likelihood with a three-dimensional Gaussian that takes into account the systematic effects, described later, in order to obtain the experimental three-dimensional likelihood for γ, δ_S, and r_S. From simulation studies we observe that, due to the small signal statistics and the high background level, r_S is overestimated and the error on γ is underestimated, when we project the experimental three-dimensional likelihood on either r_S or γ, after integrating over the other two variables. This problem disappears if either r_S is fixed in the fit or if we combine the three-dimensional likelihood function (γ, δ_S, r_S) obtained from this data sample with external information on r_S. In the following we will show the results of both these approaches.

The systematic uncertainties, summarized in Table I, are evaluated separately on γ, δ_S, and r_S and considered uncorrelated and Gaussian. It can be noted that the systematic error is much smaller than the statistical one. The systematic uncertainty from the Dalitz model used to describe true $D^0 \to K_S\pi^+\pi^-$ decays is evaluated on data by repeating the fit with models alternative to the nominal one, as described in detail in [5]. The $D^0 \to K_S\pi^+\pi^-$ Dalitz model is known to be the source of the largest systematic contribution in this kind of measurement [5,6]. All the other contributions have been evaluated on a high statistics simulated sample in order not to include statistical effects. To evaluate the contribution related to $m_{\rm ES}$, $\mathcal{F}$, and Δt PDFs, we repeat the fit by varying the PDF parameters obtained from MC within their statistical errors. To evaluate the uncertainty arising from the assumption of negligible peaking background contributions, the true D^0 fraction and $R_{b\to u}$ in the background, we repeat the fit by varying the number of these events and fractions within their statistical errors. The uncertainty from the assumptions on the factor k is also evaluated. The reconstruction efficiency across the Dalitz plane for true D^0 events and the Dalitz plot distributions for background with no true D^0 have been parametrized on MC using polynomial functions. Systematic uncertainties have been evaluated by repeating the fit assuming the efficiency and the distribution for these backgrounds to be flat across the Dalitz plane.

TABLE I. Systematics uncertainties on γ, δ_S, and r_S.

Systematics source	$\Delta\gamma[^o]$	$\Delta\delta_S[^o]$	$\Delta r_S(10^{-2})$
Dalitz model for signal	6.50	15.80	6.00
PDF shapes	1.50	2.50	5.20
Peaking background	0.14	0.12	0.04
k parameter	0.07	1.20	7.10
True D^0 in the background	0.05	0.03	1.00
$R_{b\to u}$	0.01	1.10	1.90
Efficiency variation	0.31	0.62	0.61
Dalitz background parameter	0.03	0.27	0.20
Total	6.70	16.10	11

In Fig. 3, we show the 68% probability region obtained for γ assuming different fixed values of r_S and integrating over δ_S. For values of $r_S < 0.2$ we do not have a significant measurement of γ. The value of (the fixed) r_S does not affect the central value of γ, but its error. For example, for r_S fixed to 0.3, we obtain $\gamma = (162 \pm 51)^\circ$. On MC, for the same fit configuration, the average error is 45° with a rms of 14°. The *BABAR* analysis for charged B decays [5], using the same Dalitz technique for $\tilde{D}^0 \to K_S\pi^+\pi^-$, gives, for a similar luminosity, an error on γ of 29°, from the combination of $B^\pm \to \tilde{D}^0 K^\pm$, $B^\pm \to \tilde{D}^{*0} K^\pm$, and $B^\pm \to \tilde{D}^0 K^{*\pm}$. The use of neutral B decays can hence give a contribution to the improvement of the precision on γ determination comparable with that of a single charged B channel.

Combining the final three-dimensional PDF with the PDF for r_S measured with an ADS method [2], reconstructing the neutral D mesons into flavor modes [10], we obtain, at 68% probability:

$$\gamma = (162 \pm 56)^\circ \quad \text{or} \quad (342 \pm 56)^\circ; \tag{6}$$

$$\delta_S = (62 \pm 57)^\circ \quad \text{or} \quad (242 \pm 57)^\circ; \tag{7}$$

$$r_S < 0.30; \tag{8}$$

while, at 95% probability:

$$\gamma \in [77, 247]^\circ \quad \text{or} \quad [257, 426]^\circ; \tag{9}$$

$$\delta_S \in [-23, 147]^\circ \quad \text{or} \quad [157, 327]^\circ; \tag{10}$$

$$r_S < 0.55. \tag{11}$$

The preferred value for γ is somewhat far from the value obtained using charged B decays, which is around 75° for

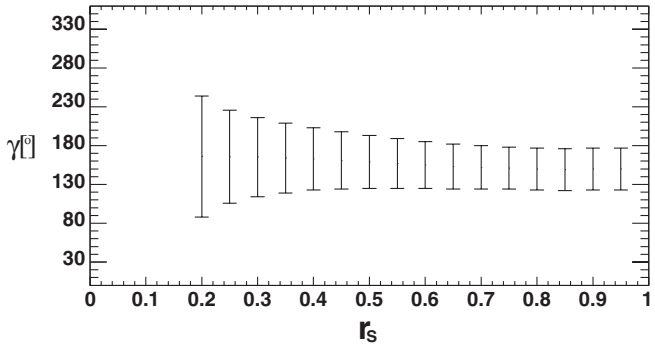

FIG. 3. The 68% probability regions obtained for γ, for different values of r_S. For values of r_S lower than 0.2, the distribution obtained for γ is almost flat and hence does not allow one to determine significative 68% probability regions. The solution corresponding to a 180° ambiguity is not shown.

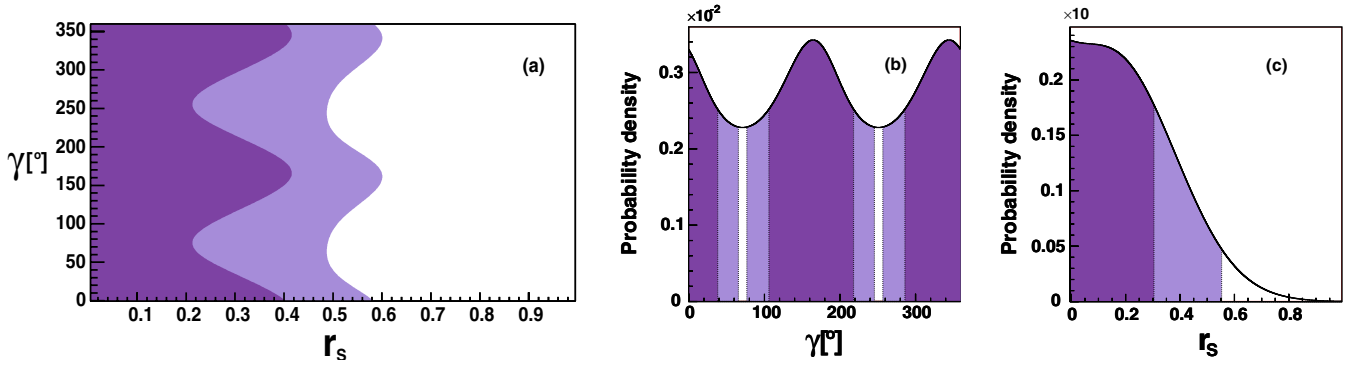

FIG. 4 (color online). The 68% (dark shaded zone) and 95% (light shaded zone) probability regions for the combined PDF projection on the γ vs r_S plane (a), γ (b), and r_S (c).

both *BABAR* and Belle Dalitz analyses, but is compatible with both the results within about 1.5σ. In Fig. 4 we show the distributions we obtain for γ, r_S, and γ vs r_S (the 68% and 95% probability regions are shown in dark and light shading, respectively). The one-dimensional distribution for a single variable is obtained from the three-dimensional PDF by projecting out the variable and integrating over the others.

VI. CONCLUSIONS

In summary, we have presented a novel technique for extracting the angle γ of the unitarity triangle in $B^0 \to \tilde{D}^0 K^{*0}$ ($\bar{B}^0 \to \tilde{D}^0 \bar{K}^{*0}$) with the $K^{*0} \to K^+\pi^-$ ($\bar{K}^{*0} \to K^-\pi^+$), using a Dalitz analysis of $\tilde{D}^0 \to K_S\pi^+\pi^-$. With the present data sample, interesting results on γ [Eqs. (6) and (9)] and r_S [Eqs. (8) and (11)] are obtained when combined with the determination of r_S from the study of $\tilde{D}^0$ decays into flavor modes. The result for γ is consistent, within 1.5σ, with the determination obtained using charged B mesons. If the ratio r_S is found to be of the order of 0.3, the use of neutral B mesons, proposed here, could give results on γ as precise as those obtained using similar techniques and charged B mesons [5].

ACKNOWLEDGMENTS

We are grateful for the extraordinary contributions of our PEP-II colleagues in achieving the excellent luminosity and machine conditions that have made this work possible. The success of this project also relies critically on the expertise and dedication of the computing organizations that support *BABAR*. The collaborating institutions wish to thank SLAC for its support and the kind hospitality extended to them. This work is supported by the U.S. Department of Energy and National Science Foundation, the Natural Sciences and Engineering Research Council (Canada), the Commissariat à l'Energie Atomique and Institut National de Physique Nucléaire et de Physique des Particules (France), the Bundesministerium für Bildung und Forschung and Deutsche Forschungsgemeinschaft (Germany), the Istituto Nazionale di Fisica Nucleare (Italy), the Foundation for Fundamental Research on Matter (The Netherlands), the Research Council of Norway, the Ministry of Education and Science of the Russian Federation, Ministerio de Educación y Ciencia (Spain), and the Science and Technology Facilities Council (United Kingdom). Individuals have received support from the Marie-Curie IEF program (European Union) and the A. P. Sloan Foundation.

[1] M. Gronau and D. London, Phys. Lett. B **253**, 483 (1991); M. Gronau and D. Wyler, Phys. Lett. B **265**, 172 (1991); I. Dunietz, Phys. Lett. B **270**, 75 (1991); Z. Phys. C **56**, 129 (1992).
[2] D. Atwood, I. Dunietz, and A. Soni, Phys. Rev. Lett. **78**, 3257 (1997); Phys. Rev. D **63**, 036005 (2001).
[3] A. Giri, Yu. Grossman, A. Soffer, and J. Zupan, Phys. Rev. D **68**, 054018 (2003).
[4] N. Cabibbo, Phys. Rev. Lett. **10**, 531 (1963); M. Kobayashi and T. Maskawa, Prog. Theor. Phys. **49**, 652 (1973).
[5] B. Aubert *et al.* (*BABAR* Collaboration), Phys. Rev. D **78**, 034023 (2008).
[6] K. Abe *et al.* (Belle Collaboration), arXiv:0803.3375.
[7] M. Gronau, Phys. Lett. B **557**, 198 (2003).
[8] M. Bona *et al.* (UTfit Collaboration), J. High Energy Phys. 07 (2005) 028; updated results available at http://www.utfit.org/.
[9] J. Charles *et al.* (CKMfitter Collaboration), Eur. Phys. J. C **41**, 1 (2005); updated results available at http://ckmfitter.in2p3.fr.
[10] B. Aubert *et al.* (*BABAR* Collaboration), Phys. Rev. D **74**,

031101 (2006).
[11] G. Cavoto *et al.*, arXiv:hep-ph/0603019.
[12] B. Aubert *et al.* (*BABAR* Collaboration), Nucl. Instrum. Methods Phys. Res., Sect. A **479**, 1 (2002).
[13] C. Amsler *et al.* (Particle Data Group), Phys. Lett. B **667**, 1 (2008).
[14] R. A. Fisher, Annals Eugen. **7**, 179 (1936).
[15] H. Albrecht *et al.* (ARGUS Collaboration), Z. Phys. C **48**, 543 (1990).
[16] B. Aubert *et al.* (*BABAR* Collaboration), Phys. Rev. Lett. **99**, 171803 (2007).
[17] E. P. Wigner, Phys. Rev. **70**, 15 (1946); S. U. Chung *et al.*, Ann. Phys. (N.Y.) **4**, 404 (1995); V. V. Anisovich and A. V. Sarantsev, Eur. Phys. J. A **16**, 229 (2003).
[18] S. Pruvot, M.-H. Schune, V. Sordini, and A. Stocchi, arXiv:hep-ph/0703292.
[19] F. Polci, M.-H. Schune, and A. Stocchi, arXiv:hep-ph/0605129.